ORIGINAL ARTICLE

Fluorine-incorporated TiO$_2$ nanotopography enhances adhesion and differentiation through ERK/CREB pathway

Hyang-Seon Ro[1] | Hee-Jung Park[2] | Young-Kwon Seo[2]

[1]Department of Chemical and Biochemical Engineering, Dongguk University, Seoul, South Korea

[2]Department of Medical Biotechnology (BK21 Plus team), Dongguk University, Gyeonggi-do, South Korea

Correspondence
Young-Kwon Seo, PhD, Department of Medical Biotechnology, Dongguk University, Pil-dong 3-ga, Chung-gu, Seoul 100-715, South Korea.
Email: bioseo@dongguk.edu

Abstract

This study compared the topography of different titanium surface structures (TiO$_2$ nanotube and grain) with similar elemental compositions (TiO2 and fluorine [F]) on the Ti surface. High magnification indicated that the surfaces of the control and etching groups were similar to each other in a flat, smooth form. The group anodized for 1 h was observed with TiO$_2$ nanotubes organized very neatly and regularly. In the group anodized for 30 min after etching, uneven wave and nanopore structures were observed. In addition, MTT assay showed that the F of the surface did not adversely affect cell viability, and the initial cell adhesion was increased in the 2.8% F-incorporated TiO$_2$ nanograin. At the edge of adherent cells, filopodia were observed in spreading form on the surfaces of the anodizing and two-step processing groups, and they were observed in a branch shape in the control and etching groups. Moreover, cell adhesion molecule and osteogenesis marker expression was increased at the F-incorporated TiO$_2$ nanostructure. In addition, it was found that the expression of p-extracellular signal-regulated kinase (ERK) and p-cAMP response element-binding protein (CREB) increased in the TiO$_2$ nanograin with the nanopore surface compared to the micro rough and nanotube surfaces relative to the osteogenic-related gene expression patterns. As a result, this study confirmed that the topographic structure of the surface is more affected by osteogenic differentiation than the pore size and that differentiation by specific surface composition components is by CREB. Thus, the synergy effect of osteogenic differentiation was confirmed by the simultaneous activation of CREB/ERK.

KEYWORDS
elemental composition, fluorine, surface topography, TiO$_2$ nanograin, TiO$_2$ nanotube

1 | INTRODUCTION

Titanium (Ti) has good mechanical, anticorrosive, and biocompatibility characteristics.[1-5] Additionally, titanium dioxide (TiO$_2$) oxide layer formation on the Ti surface provides excellent anti-corrosive and

biocompatibility properties. When Ti devices are implanted in vivo, the surrounding tissue comes into direct contact with the Ti surface. Because of this, the biocompatibility or failure cases of Ti devices depend on the characteristics of this surface layer, such as structure, chemical composition, elemental composition, and topography.[6-11]

Many investigators have shown that bioactive Ti surfaces can be induced by special chemical, physical, and thermal treatments. Various treatment techniques have been used in an effort to increase the attachment and integration of bone tissues on the implant surface by creating a rough surface, such as coating, etching, and anodizing.[12-19] In one of the known etching techniques, acid or alkaline solution and thermal treatment creates a macroporous and rough titanate layer on the surface of Ti, and it can induce bone-like mineral deposition in vivo fluid.[12,16,18] Moreover, electrochemical techniques have been used to create TiO_2 nanostructures on Ti surfaces by electrolytes (HF or NaOH).[14,20] Related research reported that the surface of porous TiO_2 nanotubes has much higher cell adhesion, proliferation, ALP activity,[21] bone sialoprotein, and osteocalcin expression than the conventional Ti surface.[22]

Many researchers have taken this one step further and studied the effects of TiO_2 nanostructures of various diameters by regulating the electrolyte composition, time, and voltage.[23-26] They studied the diameter effects of TiO_2 nanotubes from 15 to 100 nm on mesenchymal stem cells (MSCs) and reported that a diameter of 15–20 nm increased adhesion, spreading, proliferation, and differentiation of cells.[27] Moreover, another researcher showed that small-diameter (30–50 nm) nanotubes increased adhesion, while larger-diameter (70–100 nm) nanotubes induced bone-forming ability by increasing alkaline phosphatase.[24] In addition, Zhang et al. fabricated TiO_2 nanotubes (diameter: 150–470 nm) and showed that the 470 nm TiO_2 nanotube induced higher proliferation of osteoblasts and that ALP activity peaked at the 150 nm diameter.[5]

However, some investigators showed that a 30–40 nm nanotube on the implant surface influenced bone formation and osseointegration by enhancing osteoblast activation in vivo.[24] As such, many in vitro and in vivo research studies on TiO_2 nanotube diameter for cell proliferation and differentiation have been reported, but the responses of cell differentiation and bone formation according to diameter size have varied.

Recently, to improve the function of Ti implants, the combination of two or more technologies, such as etching, anodizing, coating, and ionization, has been attempted. Li et al. showed that BMP-2-coated TiO_2 nanotubes increased osteogenesis by inducing ALP activity.[28] Lai et al. reported that an osteogenic growth peptide coating on TiO_2 nanotubes increased the expression of collagen, Runx-2, OPN, and OC and mineralization.[29] Moreover, many studies have reported that cell proliferation and differentiation are improved by the doping of Mg, Sr, and F ions on the nano surface.[29-31] Ding et al. studied the effect of nanotube diameters (30–80 nm) on the surface with the sandblasting with grit and acid etching (SLA) method. They reported that SLA/nanotube was favorable for promoting the activity of osteoblasts compared to the only-SLA group. In addition, cell adhesion and proliferation were increased in SLA/30 nm, but cell adhesion and osteogenic gene expression were increased in SLA/80 nm.[32]

Most of the biomolecules or cytokines induce osteogenesis through the cAMP response element-binding protein (CREB) pathway. Investigators reported that anti-osteoporosis agents, BMP, pyrazole-pyridine, and osthole stimulate osteoblast differentiation and increase ALP activity, mineralization, and bone formation in vivo by activating the cAMP/PKA/CREB signaling pathway.[4] However, according to another research group, the osteogenic differentiation or induction mechanism of nanotube topographic structures is due to the extracellular signal-regulated kinase (ERK) signaling pathway. The magnesium ion/Zn-incorporated titania nanotube led to more accelerated expression of osteogenic-related genes and ECM-mineralized nodules than that on the Ti surface.[29] In addition, Dou reported that tantalum alloy activates the MAPK/ERK signaling pathway to regulate the high expression of osteogenic genes and promote the greater osteogenic differentiation of BMSCs than that on Ti.[33]

However, most of the nanotopography research has been focused on the nano size, and there have been few studies comparing physical topography and amount of chemical components/elements on the surface and cell behaviors.

Therefore, in this study, we compared physically different Ti surfaces (TiO_2 nanotube and nanograin with nanopore) with similar chemical compositions, TiO_2 and fluorine (F), on the Ti surface by examining the effect on cell adhesion, proliferation, and differentiation.

In addition, in order to identify the bone differentiation mechanism, a well-known pathway of osteogenesis was studied.

2 | MATERIALS AND METHODS

2.1 | Preparation of Ti discs

Ti discs were donated (MEGAGEN Implant Co, Korea), and substrates were 1-mm-thick discs sliced (10-mm diameter). These discs were used as a control group, and the sample was measured and analyzed three times (n = 3). The experimental group was divided into the etching, anodizing, and anodizing after etching groups and compared with the control group. Ti discs of the same size were used in both the control and experimental groups.

2.2 | Etching of TiO_2 thin film

The etching was performed by modifying previous experimental methods.[34] The Ti discs were etched in Kroll's reagent (4.0% hydrofluoric acid, 7.2% HNO_3, and 88.8% water) for 10 min with sonication at room temperature, and the etching reaction was terminated by the addition of 10 N NaOH to Kroll's reagent. These Ti discs were cleaned by sonication in dichloromethane for 10 min and then washed ultrasonically for 10 min, once in acetone and once in triple-distilled water. They were then placed in 40% HNO_3 for 40 min to passivate the surface of the Ti discs.[34] The acid-etched Ti discs were then rinsed with distilled water, followed by thermal treatment at 400°C for 1 h.

2.3 | Anodizing for TiO$_2$ nanotube formation

The anodizing was performed by modifying previous experimental methods.[35] The anodizing electrolyte was a mixture of 99.9% ethylene glycol, 0.5% NH$_4$F, and 0.2% water. After cleaning in ethanol and acetone, the electrochemical anodizing experiments were conducted at room temperature. The Ti discs were anodized for 1 h at 30 V in anodizing electrolyte mixture using a DC power supply at 25°C in a 60% humidified atmosphere.

2.4 | Second step of surface modification through anodizing after etching

The second step of surface treatment was performed by modifying previous experimental methods.[34,35] The Ti discs were etched by sonication in Kroll's reagent for 10 min at room temperature, and the etching reaction was terminated by the addition of 10 N NaOH to Kroll's reagent. These Ti discs were cleaned by sonication in dichloromethane for 10 min, washed ultrasonically for 10 min, and placed in 40% HNO$_3$ for 40 min to passivate the surface of the Ti discs. Then, the acid-etched Ti discs were rinsed with triple-distilled water. After drying in a vacuum oven, the Ti discs were anodized for 30 min at 30 V in an anodizing electrolyte mixture (99.9% ethylene glycol, 0.5% NH$_4$F, and 0.2% water) using a DC power supply at 25°C in a 60% humidified atmosphere.

2.5 | Cell adhesion assay

Human bone marrow mesenchymal stem cells (BM-MSCs) were purchased from Lonza (Walkersville, MD, USA). During expansion, the MSCs were cultured with Dulbecco's Modified Eagle Medium (DMEM, Welgen, Korea) with 10% fetal bovine serum (FBS, Lonza Ltd., Switzerland) and 1% penicillin at 37°C in an incubator (5% CO$_2$ and 95% humidified atmosphere), and the medium was changed three times a week. BM-MSCs were seeded on Ti surfaces at an initial density of 2×10^4 cells and left to adhere for at least 24 h and to culture for 72 h with osteogenic differentiation medium.

Cell adhesion was analyzed using MTT assay.[34] Cell-cultured discs were washed with PBS, and 1 ml of a 0.5 mg/ml-MTT supplemented cell culture medium was added at 37°C and 5% CO2 for 1 h. The MTT solution was removed after 1 h; then, 1 ml of DMSO was added, and it was shaken for 10 min. The intense purple-colored formazan derivative formed during active cell metabolism was eluted, and absorbance was measured at 540 nm.

2.6 | Analysis of Ti surface

In order to examine the difference in the surface structure, surface analysis was carried out by scanning electron microscopy (SEM, JSM-7001F, JEOL Ltd, Japan), energy dispersive X-ray (EDX, JSM-7001F, JEOL Ltd, Japan), and X-ray photoelectron spectroscopy (XPS, ESCALAB 220i-XL,

VG Scientific Instruments). In addition, the surface hydrophilicity of TiO$_2$ was studied by measuring the static contact angle with a sessile drop of distilled water deposited on the sample surface.[35] The volume of the liquid was kept constant (10 μl), and each contact angle value was the average of five measurements at room temperature.

2.7 | Reverse transcription polymerase chain reaction

The mRNA levels of osteogenesis-related genes were assessed by reverse transcription polymerase chain reaction (RT-PCR). The cells were seeded at 1×10^5 cells on Ti surfaces and harvested after being cultured for 3 days using TRIzol (Invitrogen, CA, USA) to extract the RNA. The harvested RNA was reverse transcribed into complementary DNA using a Prime Script RT Reagent Kit. The PCR was conducted by subjecting the samples to 21–35 cycles of denaturation (94°C, 1 min), annealing (53–57°C, 1 min), and extension (72°C, 1 min). The samples were then placed on 2% agarose gel and visualized by SYBR Safe DNA gel staining (Invitrogen Co., USA). The relative abundance of transcripts of GAPDH, type I collagen, BMP-2, Runx-2, ALP, and vimentin was measured. The primers for the target genes are listed in Table 1.

2.8 | Western blotting

The proteins were extracted from cultured cells, and the concentrations were evaluated using the BCA method. Samples of 25 μl (20 μg total protein) were separated using 30% SDS polyacrylamide gel electrophoresis and transferred onto PVDF. Then, membranes were incubated with blocking solution (48 mM Tris, 39 mM glycine, 0.05% SDS, 5% methanol) at room temperature for 1 h. Proteins were detected with human anti-β-actin, anti-VCAM, anti-ALCAM, anti-P-selectin anti-osteocalcin, anti-osteonectin, anti-osteoprotegerin, anti-bone sialoprotein, anti-versican, anti-BMP-2, and anti-ERK antibodies at 4°C overnight and with anti-human secondary antibodies for 2 h at room temperature. The membranes were rinsed in 1X TBS and labeled as ECL substrates, and then protein bands were analyzed using the Fluor-S Gel Imaging Analysis System.

TABLE 1 Primers used for RT-PCR

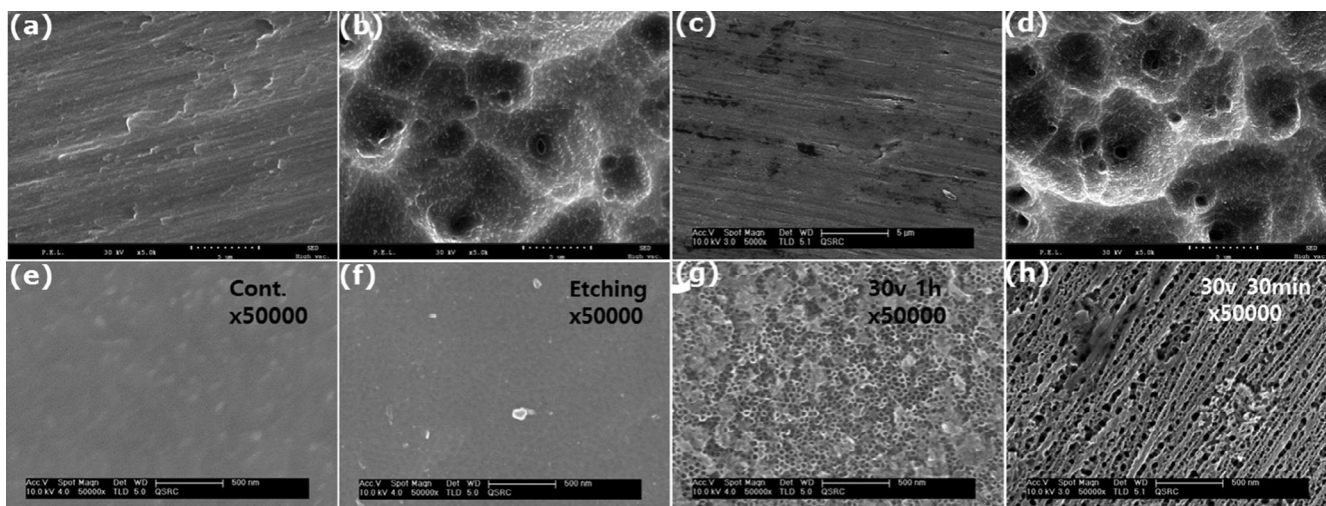| Gene	Primer sequence	Temp.(°C)	Cycle
Vimentin	F: GGAACAGCATGTCCAAATCG R: TCAGTGGACTCCTGCTTTGC	57	23
Collagen I	F: GAAAACATCCCAGCCAAGAA R: CAGGTTGCCAGTCTCCTCAT	56	32
Runx-2	F: CTCACTACCACACCTACCTG R: TCAATATGGTCGCCAAACAG	56	35
BMP-2	F: AACCTACAACCCCACCACAA R: GTTCCCCTGTCTCACTTTCA	57	32
GAPDH	F: ACCACAGTCCATGCCATCAC R: TTCACCACCCTGTTGCTGTA	55	25

FIGURE 1 Comparison of structure of surface-modified Ti by SEM images. (a,e) Untreated raw Ti surface showing nearly smooth surface, (b,f) Etched Ti surface, (c,g) Anodized (for 1 h at 30 V) Ti surface, (d,h) Anodized (for 30 min at 30 V) Ti surface after etching (a–d: × 5,000, e–h: × 50,000)

2.9 | Statistical analysis

Data on cell growth and cytokines were statistically evaluated using Student's t test. The difference between means was considered significant when $p < 0.05$.

3 | RESULTS

3.1 | Comparison of Ti surface structure

As a result of surface observation with SEM, the structure of the etched Ti disc surface contained microporous puddle surface features (Figure 1b). However, anodization, which was carried out for 1 h in NH_4F at 30 V, resulted in a Ti substrate showing regular scratch marks at low magnification (Figure 1c). Moreover, after etching, the anodization with the same concentration of NH_4F at 30 V for 30 min resulted in a Ti surface very similar to that of the etched surface at low magnification (Figure 1d). At high magnification, the control and etched surfaces were very similar to each other, showing a very smooth and flat form (Figure 1e,f). Moreover, the surface of the TiO_2 nanopore structure appeared very clear, regular, and uniform after the anodization that was carried out for 1 h (Figure 1g). However, the 30-min anodizing process formed an uneven and wavy nanograin with nanopore structure (Figure 1h). In these results, the diameter of the nanotube is approximately 30–40 nm, and uniform and parallel nanotubes can be observed in these micrographs, but the nanograin is approximately 60–100 nm and the nanopore size is not uniform.

3.2 | Assay of contact angle and MTT

Many of the physical or chemical surface modifications can change the hydrophilicity of materials. After chemical and physical treatment, the water contact angles varied on the Ti surface by surface modification in this study. The untreated and etched Ti had contact angles of 88° and 77°, respectively, while the anodized Ti and the Ti anodized after etching had contact angles of 33° and 35°, respectively (Figure 2a). Therefore, it was observed that hydrophilicity was increased by anodizing rather than etching in this study.

In addition, the adhesion ratio of BM-MSCs, evaluated by MTT assay after 24 and 72 h culture, indicated a slight increase in the adhesion of cells (Figure 2b). The results after 24 h culture can be interpreted as initial adhesion, with surface treatment groups relative to control showing an increase in adhesion of about 25–60%. However, after 72 h culture, the growth rates were mostly similar, and it showed that there was an increase of about 30% compared to initial attachment.

3.3 | Comparison of cell morphology

Figure 3 presents SEM micrographs of the adhered MSCs on the various Ti surfaces after 72 h of incubation time. All the MSCs were polygonal and well distributed, and the attached morphologies were not very distinct on the various modified surfaces, but there was a noticeable difference in the number of cells attached (Figure 3a–d). However, the high-magnification image of hMSCs on the various Ti surfaces showed that the morphologies of hMSCs on the surfaces of TiO_2 nanostructures were somewhat different (Figure 3c,d). The hMSCs on nano TiO_2 showed more round lamellipodia and fewer filopodia, and regular and directional extensions were apparent on the nanotube structures even after 72 h of culture (Figure 3c). It can be assumed that the interplay between the cell and the nanostructure allows for enhanced differentiation and an overall increase in osteogenic differentiation, as indicated by the filopodia and morphology. In addition, it is suggested that F and nanograins play an important role in the adhesion and differentiation of cells. The above results show that the structure and elements of the surface affect adhesion but not
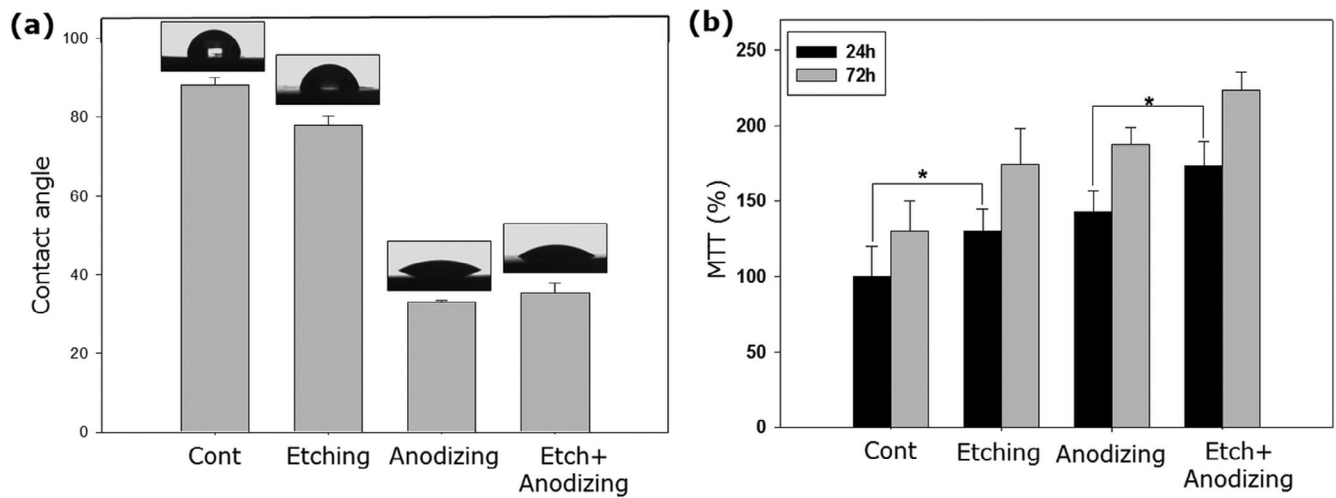
FIGURE 2 Comparison of contact angles and MTT assay on various Ti surfaces. The contact angles of the untreated surface, etched surface, anodized surface, and anodized surface after etching are $77.94 \pm 2.3°$, $77.94 \pm 2.3°$, $33.1 \pm 0.4°$, and $35.32 \pm 2.6°$, respectively. (*$p < 0.05$)
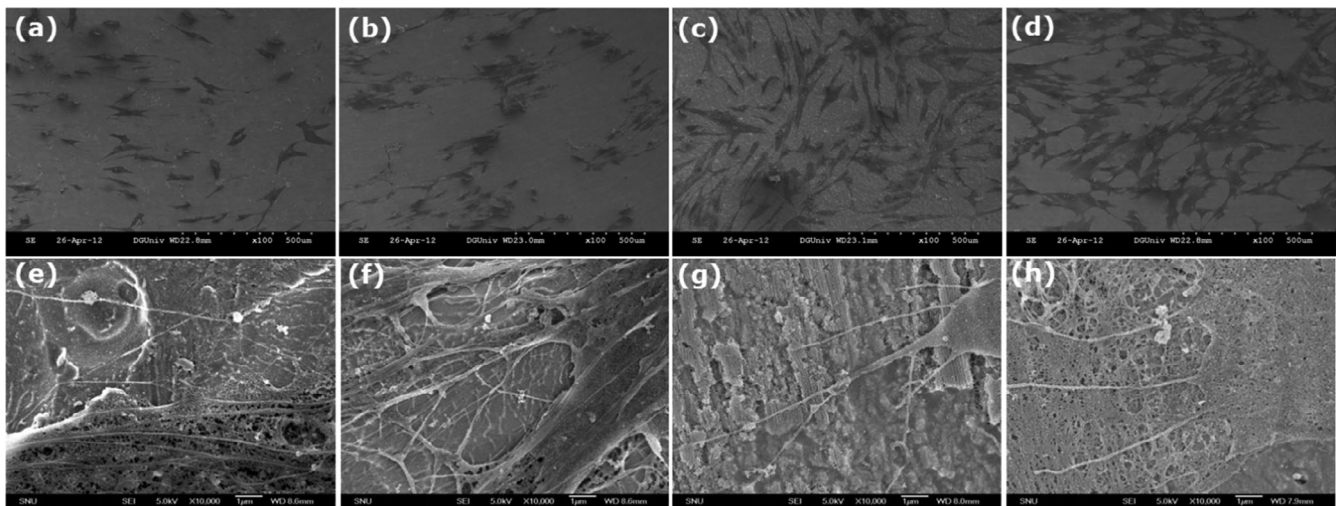

FIGURE 3 Scanning electron microscopy images of the morphologies of MSC culture on various titanium surfaces for 72 h. (a,e) Untreated raw Ti surface showing a nearly smooth surface, (b,f) Etched Ti surface, (c,g) Anodized (for 1 h at 30 V) Ti surface, (d,h) Anodized Ti surface (for 30 min at 30 V) after etching (a-d: × 100, e-h: × 10,000)

proliferation. Therefore, these F-incorporated TiO_2 nanograins with nanopore structures probably had increased initial cell adhesion (Figure 3).

3.4 | Expression of cell adhesion molecules

In this study, after surface modification, we analyzed the expression of cell adhesion molecules, including VCAM, ALCAM, and p-selectin. From the results of this analysis, the levels of VCAM, ALCAM, and p-selectin were significantly higher in MSCs cultured in the anodized and two-step modification groups than in those in the other groups, but the VCAM protein phosphorylation level in the two-step modification group was similar to that of the anodizing group. In particular, the level of ALCAM was significantly

higher in the two-step modification group compared to the other groups. In other words, the protein levels involved in cell adhesion were generally increased by the anodized and two-step modification treatments. These results show that TiO_2 nano and micro topography, rather than a smooth surface, plays an important role in improving cell adhesion (Figure 4).

3.5 | Analysis of elements

In the surface chemistry characterization, we analyzed the different chemistries among the various Ti samples fabricated in this study (Figure 5). Most significantly, unlike all other samples, the unmodified Ti did not have any F present on the surface, since the etching or anodization electrolyte solution contained F. Depending on the
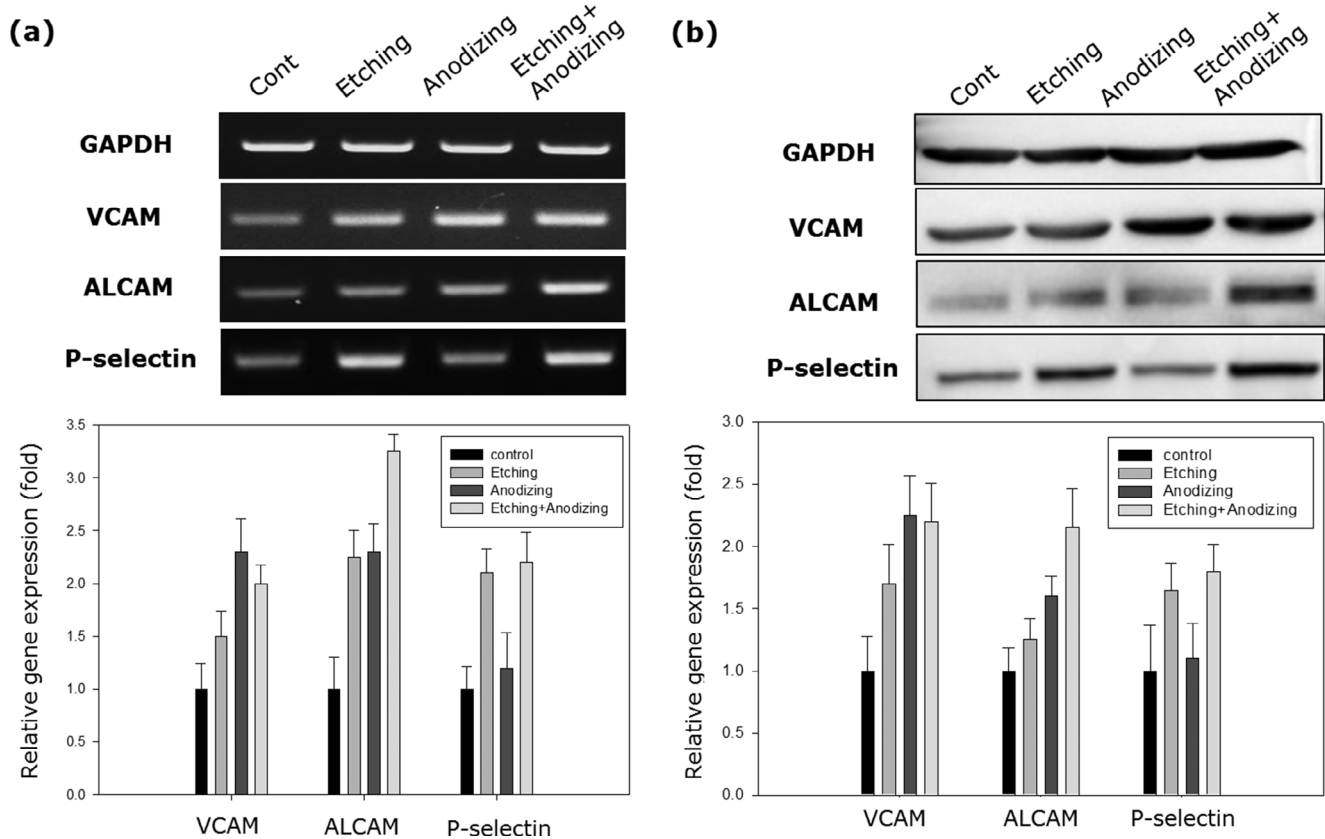
(a)

(b)

FIGURE 4 Expression cell adhesion molecule mRNA (a) and protein (b) in BM-MSCs on various Ti surfaces. The levels of all markers were significantly increased in the anodized and anodized after etching groups

surface treatment process, the amount of carbon (C) and Ti was reduced, and the amount of oxygen (O) and F was increased, indicating that a TiO_2 thin film was formed by etching and a TiO_2 nanotube was formed by the anodizing process (Table 2). Additionally, the relative atom concentrations (at.%) and binding energies (BE) of C, O, F, and nitrogen (N) were analyzed, and the results are shown in Table 3. The C and N were analyzed as being lower for the anodized surface compared with the untreated and etched surfaces, while the O and F were estimated to be higher for the anodized surface compared with the untreated and etched surfaces. This result is similar to the trends seen in EDX analysis, whereby the surface treatment reduced the amount of C and Ti and increased the amount of O and F.

3.6 | Evaluation of effect of surface modification on cell differentiation

We also evaluated RT-PCR and western blot analysis to determine how the various surface modification methods affected osteogenic differentiation, and the analysis of the bone-related markers was performed after a 3-day culture with differentiation medium.

Versican, osteonectin, BMP-2, osteoprotegerin, and bone sialoprotein genes are important markers for different osteogenic periods, and they were used to indicate the state of the Ti surface modification-induced differentiation of MSCs in this work.

The results of this study showed that the mRNA expression levels of BMP-2, Runx-2, ALP, and vimentin were significantly increased, and the protein levels of versican, osteonectin, BMP-2, osteoprotegerin, osteocalcin, and bone sialoprotein were significantly increased in the F-incorporated TiO_2 nanograin. The expression levels of most mRNAs and proteins were increased in the nano surface (anodized and two-step modification) groups (Figure 6).

Osteonectin is a glycoprotein in the bone that binds sodium, and it initiates mineralization and promotes mineral crystal formation. Moreover, osteocalcin, osteoprotegerin, and BMP-2, similar to other bone morphogenetic proteins, play an important role in the development of bone and cartilage. Osteocalcin protein is specifically synthesized by osteoblasts, and it is a marker of osteoblast differentiation during the later stages of bone formation,[36] and MSCs produce a soluble glycoprotein called osteoprotegerin.[37] In addition, BMP-2 induces osteoblastic differentiation by acting directly on MSCs, and it is used clinically to induce bone formation, although high doses are required.[32] Moreover, bone sialoprotein is a highly post-translationally modified acidic phosphoprotein normally expressed in mineralized tissues, such as bone and dentin.[38]

It is well known that ERK and CREB are closely related to the osteogenic differentiation of stem or progenitor cells. In this study, the relevance of surface structures and elements was analyzed, and it was found that the expression of p-ERK and p-CREB increased in the etching/anodizing groups compared to the anodizing or etching groups relative to the osteogenic-related gene expression patterns. In
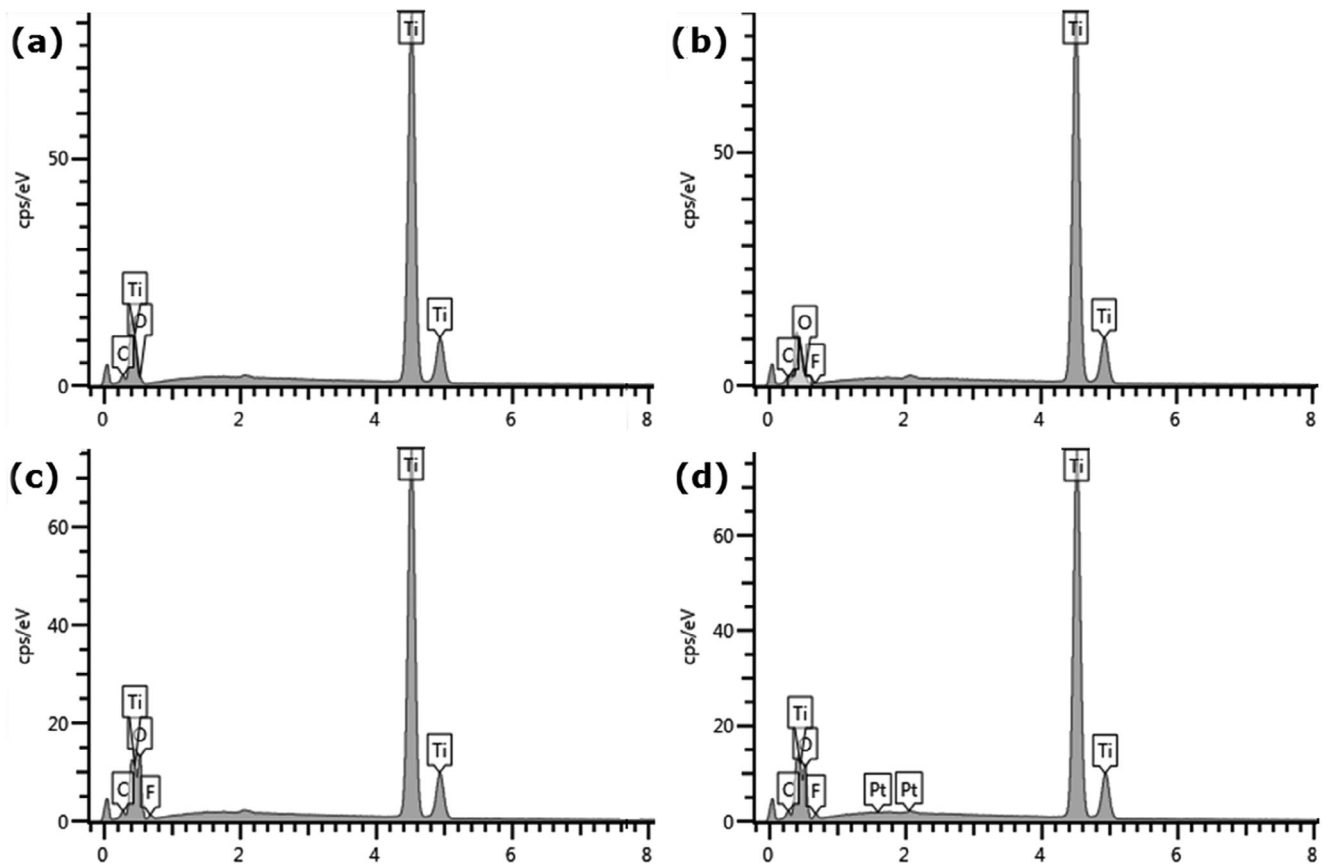
FIGURE 5 EDX analysis of various Ti surfaces (a) Untreated raw Ti surface showing nearly smooth surface, (b) Etched Ti surface, (c) Anodized (for 1 h at 30 V) Ti surface, (d) Anodized (for 30 min at 30 V) Ti surface after etching

TABLE 2 Energy dispersive X-ray spectroscopy (EDX) analysis of top surface

Element	wt%			
	Untreated Ti	Etched Ti	Anodized Ti	Anodized after etch Ti
C	4.04	3.16	2.32	2.55
O	0.86	5.08	30.68	27.48
F	0	0.37	1.93	2.46
Ti	95.1	91.39	65.07	67.51
Total	100	100	100	100

TABLE 3 Binding energies and at.% of elements in XPS analysis

Surface	C		O		F		N	
	at.%	BE	at.%	BE	at.%	BE	at.%	BE
Untreated Ti	25.4	284.8	53.9	529.9	—	—	2.3	399.8
Etched Ti	26.6	284.9	50.9	530.0	—		1.1	399.9
Anodized Ti	16.7	285.1	58.7	530.0	1.9	684.1	—	—
Anodized after etch Ti	20.7	285.1	58.0	530.0	2.8	684.4	0.3	399.4

Abbreviations: at.%, atom concentration rate; BE, binding energy; XPS, X-ray photoelectron spectroscopy.

other words, the enhancement of osteogenic differentiation by the amount of nano surface and F was found to occur through the ERK/CREB pathway (Figure 7).

In conclusion, cell activity increased by 30–40% when the contact angle of the Ti surface increased, and attachment molecules at the gene and protein levels were also observed to be more than twice as
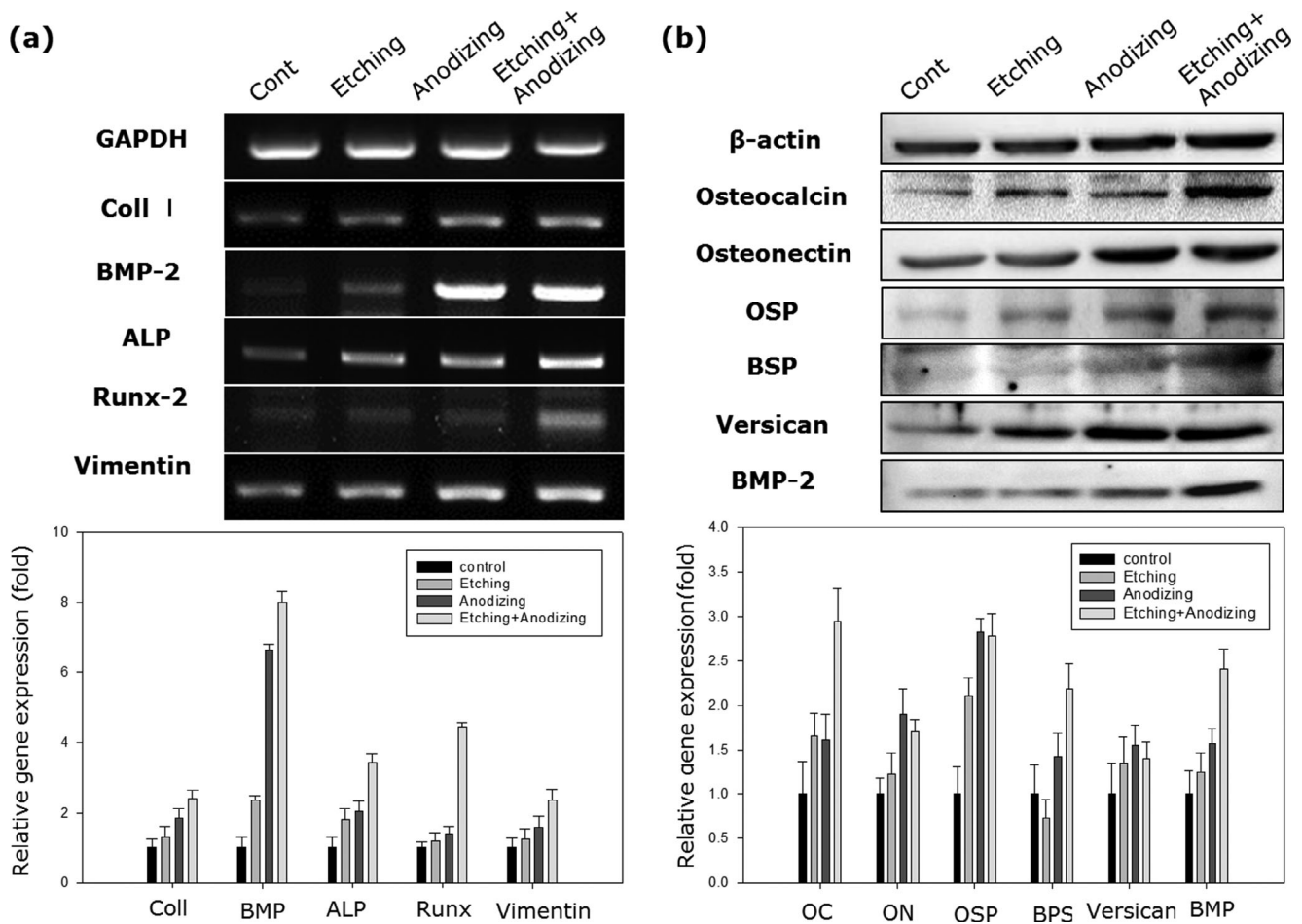
FIGURE 6 Expression of osteogenic-related transcriptional factors (a) and protein in BM-MSCs on various Ti surfaces (b) for 72 h

strong. In this study, only qualitative analysis was performed on the Ti surface structure. However, it was confirmed that cell growth and ALCAM adhesion molecules also increased as the components of F and O on the surface increased from the anodizing group at 1.9(wt%) and the etching/anodizing group at 2.46(wt%) compared with the control. Moreover, CREB expression increased with the increase in F components on the Ti surface. Thus, nanostructure topography can positively affect cell adhesion and differentiation, and the composition of the elements plays an important role in osteogenesis.

4 | DISCUSSION

Cell adhesion, growth, and differentiation are important parameters by which implant surfaces can be evaluated for their biocompatibility. In addition, a stable connection between the implant surface and the surrounding tissue is one of the most important prerequisites for the long-term success of medical devices.

Thus, implant surface modification techniques have been studied by many researchers. In particular, with the development of nanotechnology, the study of nano surface formation has come into the spotlight. It is well known that nanopore diameters

depend on the electrolyte ingredients, anodizing time, and potential.[39,40]

Kim et al. demonstrated the excellence of SLA/anodizing surfaces through cell culture under various experimental conditions in which Ti was treated with SLA, anodizing, and anodizing over SLA. Another researcher compared the SLA surface with the SLA/anodizing surface (diameter: 30–80 nm) and reported improvement of cell adhesion and osteogenesis in the SLA/anodizing group.[32] The increased cell activity in vitro and osseointegration in the animal transplantation of SLA/anodizing nano surfaces rather than SLA can be interpreted as a synergistic effect of geometry. However, it is insufficient to explain that even on surfaces with microtubules on SLA surfaces, in vitro cell activity and in vivo osseointegration increase. In other words, when a structure forms a microtubule (0.5–3 μm) over a micro rough surface (2–4 μm), this is a topographic synergistic effect.

Therefore, our study examined the topographic differences of the surface and focused on the components of the surface for the adhesion and differentiation of cells. First, a microstructure was formed through the etching method, and the anodizing method was used to form a nanotube surface. On the other hand, the etching and anodizing methods were carried out sequentially to form nanostructures above the microstructure. However, the resulting
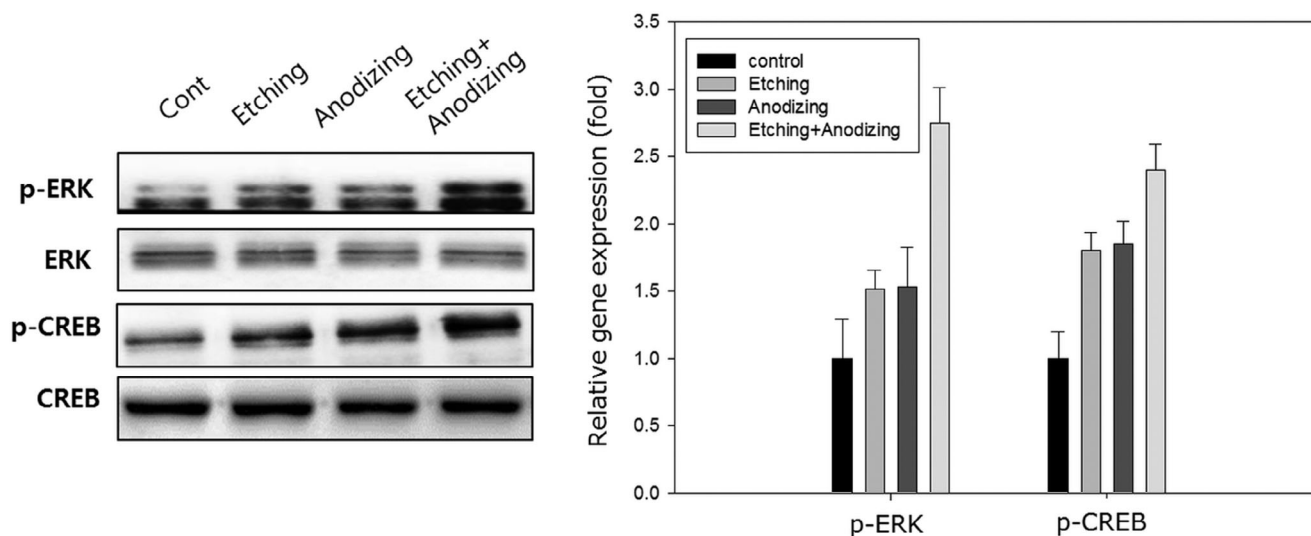
FIGURE 7 Expression of ERK and CREB genes in BM-MSCs on various Ti surfaces for 72 h

surface nanostructure was formed by grain-type 100-nm-wide porous structures rather than nanotubes (Figure 1g,h). In this work, the width of the nanotube was approximately 50–60 nm, while the inner diameter was approximately 30–40 nm, which matched the top surface morphology of the surface well at anodizing running times of 60 min, but the other surface formation was not observed at 30 min running times.

Surface treatment through etching and anodizing, respectively, formed structures similar to those found in relevant studies.[34,35] However, as a result of the short (30 min) anodizing process, nanotubes were not formed, and nanopores were formed irregularly. This is thought to have formed an early form of structure in which nanotubes are formed due to the short anodizing time.

The results of the contact angle analysis after various surface treatments showed that hydrophilicity was increased by anodizing (nano surface) rather than etching (micro surface) in this study, and similar contact angle results were observed for nanotubes and nanopore with grain surfaces. Anodizing with a nano surface was observed to increase hydrophilicity rather than etching with a micro surface. We also observed contact angles similar to those of the anodizing group on surfaces that included both nanotube and nanograin forms. Reducing the contact angle on anodizing surfaces has already been reported to increase hydrophilicity due to increased surface roughness compared to SLA surface treatment.

Our study evaluated a combination approach using MTT assays that provide the cell activity and potential cytotoxic effects by surface structures. The results showed that the various structures of the surface did not induce cell toxicity and that these nanotube structures increased initial cell adhesion at 24 h.

In our results, the increase of initial adhesion in the nanostructure over the microstructure can be interpreted as an effect of increased hydrophilicity. However, it cannot be interpreted that the topological structure that formed the grain-type nanopore with the surface of the nanotube showed similar contact angle results, causing the adhesion

of cells to improve by hydrophilicity alone. Other researchers reported a slight increase in cell adhesion in a 30-nm nanotube over SLA, but 50–80-nm nanotubes showed a similar rate of adhesion to SLA. This can be interpreted as an effect of the size of the nanotube.[32] However, our nanotubes were 30–40 nm in inner diameter and the nanopores were irregular but more than 50 nm in size. Therefore, our results regarding the effect of diameter are difficult to interpret.

In addition, in our study, the MTT analysis results at 72 h were measured for cell proliferation at about 25% relative to the initial adhesion rate under various surface conditions. This is interpreted not as a structural effect of cell proliferation on various surfaces but as an effect of proteins such as serums adsorbed to the Ti surface.

It is well known that the initial adhesion of cells is related to adhesion molecules. In this study, an analysis of the attached cells confirmed the expression of the adhesion molecules VCAM, ALCAM, and p-selectin, which was shown to have increased in the order of etching/anodizing > anodizing > etching, relative to the initial attachment rate (Figure 4).

The level of VCAM, which is constitutively expressed on BM-MSCs, follicular dendritic cells, activated endothelial cells, and skeletal muscle cells, was significantly higher in the anodizing and anodizing after etching groups than the other groups.[41] Moreover, the level of ALCAM was higher in the anodizing after etching group than in the other groups according to the western blotting results, and it has been known to play a role in the process of osteogenic differentiation.[42,43] In addition, the level of p-selectin was increased in the etching and anodizing after etching groups. The function of p-selectin as a mediator of platelet adhesion to circulate MSCs is well known,[44] and more recently, the role of p-selectin in the adhesion of MSCs to an activated endothelium has also been reported.[45]

As a result of the above, an EDX and XPS surface analysis was conducted to find other reasons besides structural differences between nanotubes and nanopores. The analysis showed that a large amount of O was measured in the anodizing group, especially with an

increased amount of F (Tables 2 and 3). It is well known that TiO_2 improves biocompatibility more than Ti. Some investigators have reported that F promotes the attachment, proliferation, and differentiation of cells.[31,37] Chen et al. performed F nano coating through PECVD processing with CF4 gas to fabricate a nano-F structure on the Ti surface. Moreover, they showed that the F-deposited Ti surface increased ALP activity and osteocalcin more than the Ti surface.[1] They doped 1, 6, and 9% F on the nano surface, respectively, and reported an increase in Runx2, ALP, BSP, OPN, and OCN from 6% as a result.[31] The results also showed that excessive F content reduces cell differentiation. In our study, we used approximately 2% F content, but the results can be interpreted as confirming that the effects of adhesion by F and cell behavior were greater than that of the surface diameter. Thus, in this study, the results for the initial attachment of cells suggest the effect of the F component present on the surface, since more F was observed in the grain-type nanopore than in the nanotube.

As a result of a comprehensive interpretation of our research and related papers and reports, we learned that a lower Ti amount and a greater amount of O and F correspond to a higher cell adhesion ratio. Moreover, it was affected more by the elements (F) of the surface than by the surface structures and topography (nanotube and pore with grain).

Thus, we hypothesize that modifying the surface of TiO_2 can increase the hydrophilicity of the Ti surface and enhance differentiation by increasing adhesion on surface-modified Ti discs. In this study, we observed that the mRNA expression of differentiation markers ALP, Runx-2, and vimentin and the protein expression of OC, ON, OSP, BSP, and BMP-2 was shown to have increased in the order of etching/anodizing > anodizing > etching, relative to the F content and adhesion ratio (Figure 6). Cooper et al. reported that fluoride modification on the TiO_2 surface enhanced cell proliferation and osteogenic differentiation through increased bone sialoprotein and BMP-2 expression.[46] Moreover, Lozano et al. reported that an F-incorporated TiO_2 nanotube of 20-nm diameter increased the proliferation, mineralization, and osteogenic gene expression of osteoblastic cells more than an F-incorporated TiO_2 nanotube of 100-nm diameter.[47] These reports show that large nanotubes are more effective at enhancing osteogenesis than small nanotubes and suggest that under the same surface topography, fluoride affects cell proliferation and differentiation.

The effects of nanostructure on osteogenic differentiation were also conformed in different morphologies. On the control and etching (microstructure) surfaces, the cells had many irregular filopodia from their leading edges (Figure 3e,f). In contrast, the MSCs on the nano surface showed a few filopodia extending from the edges of lamellipodia (Figure 3g,h). The relationship between the morphological changes and differentiation of these cells has been shown in relevant studies.[48,49] They revealed that cells were widespread and there were many filopodial interactions with the surface in the initial period but that the cell spreading area declined, the number of lamellipodia reduced, and the cell height increased when osteogenesis was induced.[48] In addition, another researcher reported that undifferentiated MSCs showed a cell surface covered by many filopodia and their morphology was changed into a bipolar fibroblastic-like shape during differentiation.[49]

In the analysis to observe the intracellular mechanism of these results, we revealed the expression of p-ERK and p-CREB, which was shown to have increased in the order of etching/anodizing > anodizing > etching, relative to the F content. This F-incorporated nano surface enhanced the responses of BM-MSCs by increasing initial adhesion and cell differentiation. Most biomolecules or cytokines induce osteogenesis through the CREB pathway. Kim et al. reported that a derivative of pyrazole-pyridine stimulates the osteoblast differentiation of human MSCs and increases bone formation in ovariectomized mice by activating the cAMP/PKA/CREB signaling pathway,[50] and Zhang et al. showed that BMP-9 promotes PKA activity and enhances CREB phosphorylation in MSCs.[4] In addition, it is known that osthole promotes osteogenesis in osteoblasts by enhancing ALP activity and mineralization through the elevation of phosphorylation of the CREB protein.[51] Chae et al. reported that fluoride stimulates rat fetal calvarial osteoblastic cell differentiation, ALP activity, and dose-dependent nodule formation through cAMP and p-CREB.[52]

On the other hand, many researchers have shown that the osteogenic differentiation or induction mechanism of nanotube structures is the ERK signaling pathway. The magnesium ion-incorporated titania nanotube accelerated the expression of osteogenic-related genes (ALP, Col-I, OCN, and RUNX2) more than that on the Ti surface,[29] and the Zn-incorporated titania nanotube increased ALP production and ECM-mineralized nodules more than that on the Ti surface through the ERK1/2 signaling pathway.[3]

Therefore, we know that the osteogenic differentiation of MSCs on F-incorporated TiO_2 nanotopography is facilitated through the ERK/CREB pathway. When looking at the above research trends, the osteogenic differentiation effect of nanopores and nanograins was enhanced through the ERK pathway, but as the western blotting results show, no difference in expression between the anodizing and etching surfaces was observed. However, the anodizing after etching treatment was able to increase ERK phosphorylation.

In addition, the effect on the osteogenesis of F was enhanced through the CREB pathway, and it was confirmed that CREB phosphorylation increased in proportion to the increase in F content (Figure 7). Moreover, the anodizing after etching treatment increased CREB phosphorylation the most.

As a result, the quality of the connection between cells and biomaterials must be considered together with the surface chemical composition and the structure of topography.

This study analyzed the effect of the topographic structure and surface composition of the Ti surface on cell adhesion and differentiation in vitro. Furthermore, in vivo experiments should be conducted to overcome the limitations of in vitro experiments and evaluate biocompatible substances accurately.

ACKNOWLEDGMENT

DATA AVAILABILITY STATEMENT

https://www.force11.org/article/fluorine-incorporated-tio2-nanotopography-enhances-adhesion-and-differentiation-through.

REFERENCES

1. Chen M, Li H, Wang X, Qin G, Zhang E. Improvement in antibacterial properties and cytocompatibility of titanium by fluorine and oxygen dual plasma-based surface modification. *Appl Surf Sci*. 2019;*463*: 261-274.

2. Das S, Gurav S, Soni V, et al. Osteogenic nanofibrous coated titanium implant results in enhanced osseointegration: in vivo preliminary study in a rabbit model. *Tissue Eng Regen Med*. 2018;*15*(2):231-247.

3. Huo K, Zhang X, Wang H, Zhao L, Liu X, Chu PK. Osteogenic activity and antibacterial effects on titanium surfaces modified with zn-incorporated nanotube arrays. *Biomaterials*. 2013;*34*(13):3467-3478.

4. Zhang H, Li L, Dong Q, et al. Activation of pka/creb signaling is involved in bmp9-induced osteogenic differentiation of mesenchymal stem cells. *Cell Physiol Biochem*. 2015a;*37*(2):548-562.

5. Zhang R, Wu H, Ni J, et al. Guided proliferation and bone-forming functionality on highly ordered large diameter TiO2 nanotube arrays. *Mater Sci Eng C*. 2015b;*53*:272-279.

6. Huang J, Zhang X, Yan W, et al. Nanotubular topography enhances the bioactivity of titanium implants. *Nanomedicine*. 2017;*13*(6):1913-1923.

7. Kim M-H, Park K, Choi K-H, et al. Cell adhesion and in vivo osseointegration of sandblasted/acid etched/anodized dental implants. *Int J Mol Sci*. 2015;*16*(5):10324-10336.

8. Lee S-Y, Koak J-Y, Kim S-K, Heo S-J. Cellular response of anodized titanium surface by poly (lactide-co-glycolide)/bone morphogenic protein-2. *Tissue Eng Regen Med*. 2018;*15*(5):591-599.

9. Shen M-J, Wang G-G, Wang Y-Z, Xie J, Ding X. Nell-1 enhances osteogenic differentiation of pre-osteoblasts on titanium surfaces via the mapk-erk signaling pathway. *Cell Physiol Biochem*. 2018;*50*(4):1522-1534.

10. Smeets, R. et al. Impact of dental implant surface modifications on osseointegration. *BioMed Res Int*. 2016;*2016*:6285620.

11. Tschernitschek H, Borchers L, Geurtsen W. Nonalloyed titanium as a bioinert metal—a review. *Quintessence Int*. 2005;*36*(7):523-530.

12. Subramani K, Pandruvada S, Puleo D, Hartsfield J, Huja S. In vitro evaluation of osteoblast responses to carbon nanotube-coated titanium surfaces. *Prog Orthod*. 2016;*17*(1):1-9.

13. Yu W, Zhang Y, Jiang X, Zhang F. In vitro behavior of mc3t3-e1 preosteoblast with different annealing temperature titania nanotubes. *Oral Dis*. 2010;*16*(7):624-630.

14. Diamanti MV, Del Curto B, Pedeferri M. Anodic oxidation of titanium: from technical aspects to biomedical applications. *J Appl Biomater Biomech*. 2011;*9*(1):55-69.

15. González M, Salvagni E, Rodríguez-Cabello JC, et al. A low elastic modulus ti-nb-hf alloy bioactivated with an elastin-like protein-based polymer enhances osteoblast cell adhesion and spreading. *J Biomed Mater Res A*. 2013;*101*(3):819-826.

16. Kokubo T, Yamaguchi S. Novel bioactive materials developed by simulated body fluid evaluation: surface-modified ti metal and its alloys. *Acta Biomater*. 2016;*44*:16-30.

17. Park J, Leesungbok R, Ahn S-J, Lee S-W. Effect of etched microgrooves on hydrophilicity of titanium and osteoblast responses: a pilot study. *J Adv Prosthodon*. 2010;*2*(1):18-24.

18. Tamilselvi S, Raghavendran HB, Srinivasan P, Rajendran N. In vitro and in vivo studies of alkali-and heat-treated ti-6al-7nb and ti-5al-2nb-1ta alloys for orthopedic implants. *J Biomed Mater Res Part A*. 2009;*90*(2):380-386.

19. Yang Y, Wang X, Miron RJ, Zhang X. The interactions of dendritic cells with osteoblasts on titanium surfaces: an in vitro investigation. *Clin Oral Investig*. 2019;*23*(11):4133-4143.

20. Huang H-H, Pan S-J, Lu F-H. Surface electrochemical impedance in situ monitoring of cell-cultured titanium with a nano-network surface layer. *Scr Mater*. 2005;*53*(9):1037-1042.

21. Oh S, Daraio C, Chen LH, Pisanic TR, Finones RR, Jin S. Significantly accelerated osteoblast cell growth on aligned tio2 nanotubes. *J Biomed Mater Res Part A*. 2006;*78*(1):97-103.

22. Kim J-H, Cho K-P, Chung Y-S, et al. The effect of nanotubular titanium surfaces on osteoblast differentiation. *J Nanosci Nanotechnol*. 2010;*10*(5):3581-3585.

23. Bauer S, Kleber S, Schmuki P. Tio2 nanotubes: tailoring the geometry in h3po4/hf electrolytes. *Electrochem Commun*. 2006;*8*(8):1321-1325.

24. Brammer KS, Oh S, Cobb CJ, Bjursten LM, van der Heyde H, Jin S. Improved bone-forming functionality on diameter-controlled tio2 nanotube surface. *Acta Biomater*. 2009;*5*(8):3215-3223.

25. Park J, Bauer S, Schmuki P, von der Mark K. Narrow window in nanoscale dependent activation of endothelial cell growth and differentiation on tio2 nanotube surfaces. *Nano Lett*. 2009;*9*(9):3157-3164.

26. Wei W, Berger S, Hauser C, Meyer K, Yang M, Schmuki P. Transition of tio2 nanotubes to nanopores for electrolytes with very low water contents. *Electrochem Commun*. 2010;*12*(9):1184-1186.

27. Park J, Bauer S, von der Mark K, Schmuki P. Nanosize and vitality: Tio2 nanotube diameter directs cell fate. *Nano Lett*. 2007;*7*(6):1686-1691.

28. Li Y, Song Y, Ma A, Li C. Surface immobilization of TiO_2 nanotubes with bone morphogenetic protein-2 synergistically enhances initial preosteoblast adhesion and osseointegration. *Biomed Res Int*. 2019; *2019*:5697250.

29. Yan Y, Wei Y, Yang R, et al. Enhanced osteogenic differentiation of bone mesenchymal stem cells on magnesium-incorporated titania nanotube arrays. *Colloids Surf B Biointerfaces*. 2019;*179*:309-316.

30. Huang Y, Shen X, Qiao H, et al. Biofunctional sr-and si-loaded titania nanotube coating of ti surfaces by anodization-hydrothermal process. *Int J Nanomedicine*. 2018;*13*:633-640.

31. Zhou J, Li B, Han Y. F-doped tio 2 microporous coating on titanium with enhanced antibacterial and osteogenic activities. *Sci Rep*. 2018;*8*(1):1-12.

32. Ding X, Zhou L, Wang J, et al. The effects of hierarchical micro/nanosurfaces decorated with tio2 nanotubes on the bioactivity of titanium implants in vitro and in vivo. *Int J Nanomed*. 2015;*10*: 6955.

33. Dou X, Wei X, Liu G, et al. Effect of porous tantalum on promoting the osteogenic differentiation of bone marrow mesenchymal stem cells in vitro through the mapk/erk signal pathway. *J Orthop Transl*. 2019;*19*:81-93.

34. Kim S-H, Park J-K, Hong J-H, et al. Increase of bm-msc proliferation using l-dopa on titanium surface in vitro. *J Biomater Appl*. 2012;*27*(2): 143-152.

35. Demetrescu I, Pirvu C, Mitran V. Effect of nano-topographical features of ti/tio2 electrode surface on cell response and electrochemical stability in artificial saliva. *Bioelectrochemistry*. 2010;*79*(1): 122-129.

36. von Wilmowsky C, Bauer S, Lutz R, et al. In vivo evaluation of anodic tio2 nanotubes: an experimental study in the pig. *J Biomed Mater Res Part B*. 2009;*89*(1):165-171.

37. Sul Y-T. Electrochemical growth behavior, surface properties, and enhanced in vivo bone response of tio2 nanotubes on microstructured surfaces of blasted, screw-shaped titanium implants. *Int J Nanomed*. 2010;*5*:87.

38. Macak JM, Tsuchiya H, Taveira L, Aldabergerova S, Schmuki P. Smooth anodic tio2 nanotubes. *Angew Chem, Int Ed*. 2005;*44*(45): 7463-7465.

39. Elices MJ, Osborn L, Takada Y, et al. Vcam-1 on activated endothelium interacts with the leukocyte integrin vla-4 at a site distinct from the vla-4/fibronectin binding site. *Cell*. 1990;*60*(4):577-584.

40. Macak J, Hildebrand H, Marten-Jahns U, Schmuki P. Mechanistic aspects and growth of large diameter self-organized tio2 nanotubes. *J Electroanal Chem*. 2008;*621*(2):254-266.

41. da Costa Martins P, García-Vallejo J-JS, van Thienen JV, et al. P-selectin glycoprotein ligand-1 is expressed on endothelial cells and mediates monocyte adhesion to activated endothelium. *Arterioscler Thromb Vasc Biol*. 2007;*27*(5):1023-1029.

42. Brändström H, Björkman T, Ljunggren Ö. Regulation of osteoprotegerin secretion from primary cultures of human bone marrow stromal cells. *Biochem Biophys Res Commun*. 2001;*280*(3): 831-835.

43. Ducy P, Desbois C, Boyce B, et al. Increased bone formation in osteocalcin-deficient mice. *Nature*. 1996;*382*(6590):448-452.

44. Schwartz Z, Simon B, Duran M, Barabino G, Chaudhri R, Boyan B. Pulsed electromagnetic fields enhance bmp-2 dependent osteoblastic differentiation of human mesenchymal stem cells. *J Orthop Res*. 2008; *26*(9):1250-1255.

45. Ganss B, Kim RH, Sodek J. Bone sialoprotein. *Crit Rev Oral Biol Med*. 1999;*10*(1):79-98.

46. Cooper LF, Zhou Y, Takebe J, et al. Fluoride modification effects on osteoblast behavior and bone formation at tio2 grit-blasted cp titanium endosseous implants. *Biomaterials*. 2006;*27*(6):926-936.

47. Lozano D, Hernández-López JM, Esbrit P, et al. Influence of the nanostructure of f-doped tio2 films on osteoblast growth and function. *J Biomed Mater Res A*. 2015;*103*(6):1985-1990.

48. Subbiah R, Suhaeri M, Hwang MP, Kim W, Park K. Investigation of the changes of biophysical/mechanical characteristics of differentiating preosteoblasts in vitro. *Biomater Res*. 2015;*19*(1):1-8.

49. Teti G, Cavallo C, Grigolo B, et al. Ultrastructural analysis of human bone marrow mesenchymal stem cells during in vitro osteogenesis and chondrogenesis. *Microsc Res Tech*. 2012;*75*(5):596-604.

50. Kim JM, Choi JS, Kim YH, et al. An activator of the camp/pka/creb pathway promotes osteogenesis from human mesenchymal stem cells. *J Cell Physiol*. 2013;*228*(3):617-626.

51. Zhang Z-R, Leung WN, Li G, et al. Osthole enhances osteogenesis in osteoblasts by elevating transcription factor osterix via camp/creb signaling in vitro and in vivo. *Nutrients*. 2017;*9*(6):588.

52. Chae H-J, Chae S-W, Kang J-S, Kim D-E, Kim H-R. Mechanism of mitogenic effect of fluoride on fetal rat osteoblastic cells: evidence for shc, grb2 and p-creb-dependent pathways. *Res Commun Mol Pathol Pharmacol*. 1999;*105*(3):185-199.